Nanopatterning by dual-ion-beam sputtering

M. Joe, C. Choi, and B. Kahng
Department of Physics and Astronomy, Seoul National University, Seoul 151-747, Korea

J.-S. Kim[a)]
Department of Physics, Sook-Myung Women's University, Seoul 140-742, Korea

(Received 9 August 2007; accepted 1 November 2007; published online 7 December 2007)

We studied the development of ordered nanopatterns during dual-ion-beam sputtering (DIBS) of Au(001) in which two ion beams that cross perpendicular to each other at their azimuth are incident on the surface at a grazing angle. In the erosion (diffusion) regime, a square-symmetric two-dimensional (2D) pattern of nanodots (holes) is formed. The 2D pattern is achieved only when the two beams are balanced in the erosion regime. In the diffusion regime, no such condition is required. The observations cannot be explained by the Kuramoto-Sivashinsky (KS) equation derived from Sigmund theory with two ion beams. © *2007 American Institute of Physics*.
[DOI: 10.1063/1.2816236]

Recently, ion-beam sputtering has been widely applied to grow self-organized nanostructures on various substrates, ranging from insulators and semiconductors to metals. For example, a hexagonal pattern of nanodots was formed on a GaSb surface by ion-beam sputtering at normal incidence.[1] If the main surface species are vacancies, nanohole arrays are observed.[2,3] In contrast, at an off-normal incidence, periodic ripples can be produced on the irradiated surfaces.[4–6] Thus far, such sputter-induced patterning has been performed using a single ion beam, which might limit the variety of nanopatterns. To achieve the goal of nanosculpturing a surface as designed, we are truly in need of removing such constraint.

Carter[7] proposed the use of dual-ion-beam sputtering (DIBS) to produce more versatile nanostructures. During DIBS, the two beams are expected to induce interference effects and produce sophisticated patterns. Recently, sputter-induced patterning using multiple ion beams has been studied.[8] However, this was a numerical study, and no experimental study has examined the idea of patterning by multiple ion-beam sputtering.

In this letter, we report the experimental realization of DIBS, in which two ion beams are simultaneously incident on Au(001) at a grazing angle and perpendicular to each other at their azimuth [Fig. 1(a)]. In the diffusion (erosion) regime, in which the energy and flux are relatively weak (strong), square-symmetric patterns of two dimensional (2D) nanoholes (nanodots) are formed along the principal crystallographic directions (ion beam directions).[9] In the erosion regime, the careful balance of the two ion beams is required to form ordered nanodot patterns. If not balanced, a ripple pattern with modulated heights along each ripple prevails. In contrast, this is not the case in the diffusion regime, possibly due to the effective diffusion kinetics of adatoms and/or vacancies that cure the imbalance between the two crossing ion beams.

We attempted to describe the present experimental results through a Bradley-Harper type of approach. However, it fails to reproduce the experimental results, suggesting that different approaches are needed.

All the experiments were carried out by a custom-built ultrahigh vacuum chamber with a base pressure of high 10^{-10} Torr. Clean Au(001) was prepared in a series of Ar^+ sputtering and annealing processes up to 730 K. The clean Au(001) revealed wide terraces separated by steps running in the densely packed [110] and $[1\bar{1}0]$ crystallographic directions [Fig. 1(b)].

During DIBS, two beams of Ar^+ ions are projected simultaneously onto the Au(001) at a grazing angle of $\theta_1 \approx \theta_2 \approx 73°$ with respect to the surface normal, while they cross each other perpendicularly at the azimuth [Fig. 1(a)]. The ion energy ϵ and ion flux f are operated in two different modes: (i) $\epsilon_1=\epsilon_2=0.5$ keV and $f=f_1+f_2\approx 15$ μA/cm^2 (1 ion/nm^2 s) and (ii) $\epsilon_1=\epsilon_2=2.0$ keV and $f \approx 52-54$ μA/cm^2 (3.3–3.4 ion/nm^2 s). The former (latter) case corresponds to the diffusion (erosion) regime.[9] Evolution of the Au(001) morphology by DIBS is observed *ex situ* using atomic force microscopy operated in contact mode.

Figures 1(c) and 1(d) show the nanopatterns that develop on the Au(001) by DIBS in the order of increasing ion fluence Ψ $(=ft)$. In Fig. 1(c), rather closely packed holes are clearly visible which have fourfold symmetry with edges running along the high-symmetry directions on average. Each hole is well defined by the four, nearly straight ridges enclosing it, indicating that the pattern develops from the crossing ripples. The inset of Fig. 1(c) shows the height-height correlation function as a function of displacement $\mathbf{d}$, defined by $G(\mathbf{d})=\langle h(\mathbf{r})h(\mathbf{r}+\mathbf{d})\rangle$, where $\langle\cdot\rangle$ denotes the spatial average. On average, the ridges in both Figs. 1(c) and 1(d) are aligned along the densely packed crystallographic directions, although the beam directions are not aligned in these directions [Fig. 1(b)]. This indicates that the nanopatterning is now governed by diffusion processes. As the ion fluence increases further [Fig. 1(d)], lateral and vertical growths of the holes are observed and quantified in terms of the wavelength λ and surface roughness $W(t)$ defined by $W(t) \equiv \sqrt{(1/L^2)\Sigma_{\mathbf{r}}[h(\mathbf{r},t)-\bar{h}]^2}$, where $\bar{h}=(1/L^2)\Sigma_{\mathbf{r}}h(\mathbf{r},t)$ and L^2 is the scanned area. The wavelength is determined from the height-height correlation function.

Figure 1(e) shows representative line profiles along the two crystallographic directions, as marked in Fig. 1(d). The periodic structures associated with the ripple pattern are clearly discernible in both directions. A noticeable feature is that the ridges have different slopes on the two opposite

a)Electronic mail: jskim@sookmyung.ac.kr.

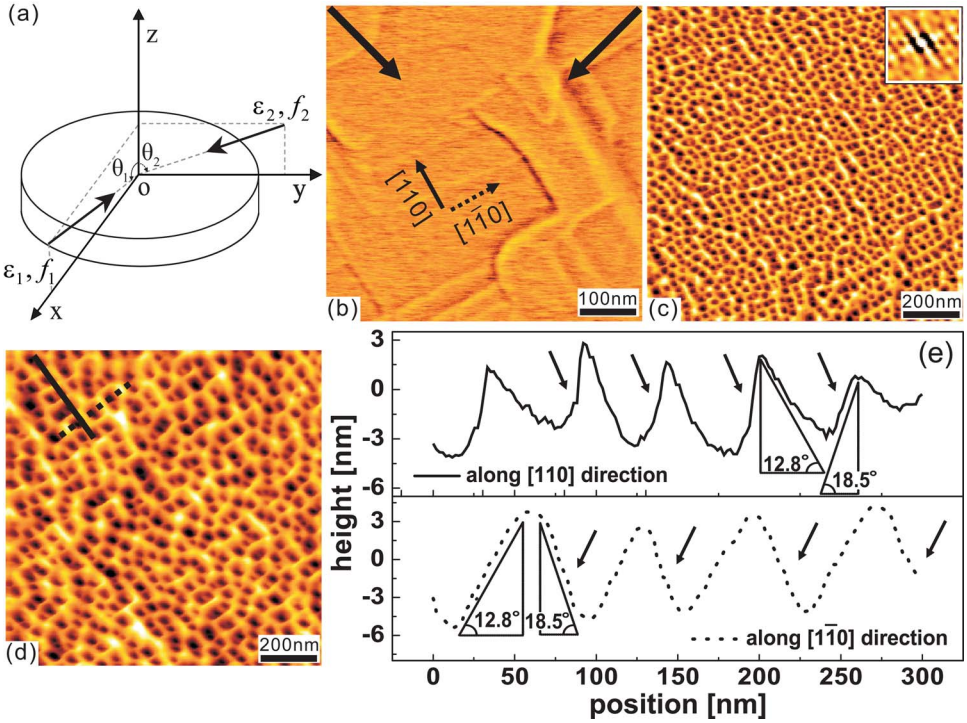

FIG. 1. (Color online) (a) Schematic illustration of the experimental geometry. (b) The initial Au(001). [(c),(d)] The surface morphologies induced by DIBS in the diffusion regime at ion fluences; (c) $\Psi=5.2\times10^3/\mathrm{nm}^2$ (t =90 min), W=15.1 Å, and λ =37–43 nm. (d) $\Psi=2.0\times10^4/\mathrm{nm}^2$ (t =330 min), W=21.2 Å, and λ =52–68 nm. (e) Height profiles along the two lines (straight for [110] and dotted for [1$\bar{1}$0] direction) marked in (d). The arrows in (b) and (e) indicate the incident ion-beam directions.

faces [Fig. 1(e)]; the illuminated (by a crossing ion beam) side is steeper than the shadowed side. This is likely a consequence of the slope dependence[10,11] of the erosion rate caused by the ion beam crossing the ripple. The nonlinear effects or slope-dependent erosion should be significant during DIBS because a beam encounters rapid variation in the slopes of the ripples crossing its path, which should significantly affect the morphological evolution and pattern formation during DIBS.

In Fig. 2, the development of an ordered pattern, now composed of nanodots, is seen along the beam directions, away from the densely packed crystallographic directions by ≈5°. Figure 2(a) shows tiny dots of varying sizes and shapes, most of which are concatenated with each other, forming a labyrinthine pattern. As the fluence increases, the dots grow, become more easily discernible from each other, and eventually form a 2D pattern, as shown in Fig. 2(b). They are fairly well ordered, showing square-symmetric correlations, yet many irregularities such as the nonuniform size and shape of nanodots bring short-range correlation of no more than 2 periods [see inset of Fig. 2(b)].

Note that in the erosion regime, unidirectional modulated ripples are usually observed [Fig. 2(c)]. The 2D pattern of the nanodots seen in Figs. 2(a) and 2(b) is achieved only after carefully balancing the two beams. In contrast, the 2D nanohole patterns in Figs. 1(c) and 1(d) are formed under a diffusion regime with no strict requirements for the balance of the two ion beams. We may understand the two distinct

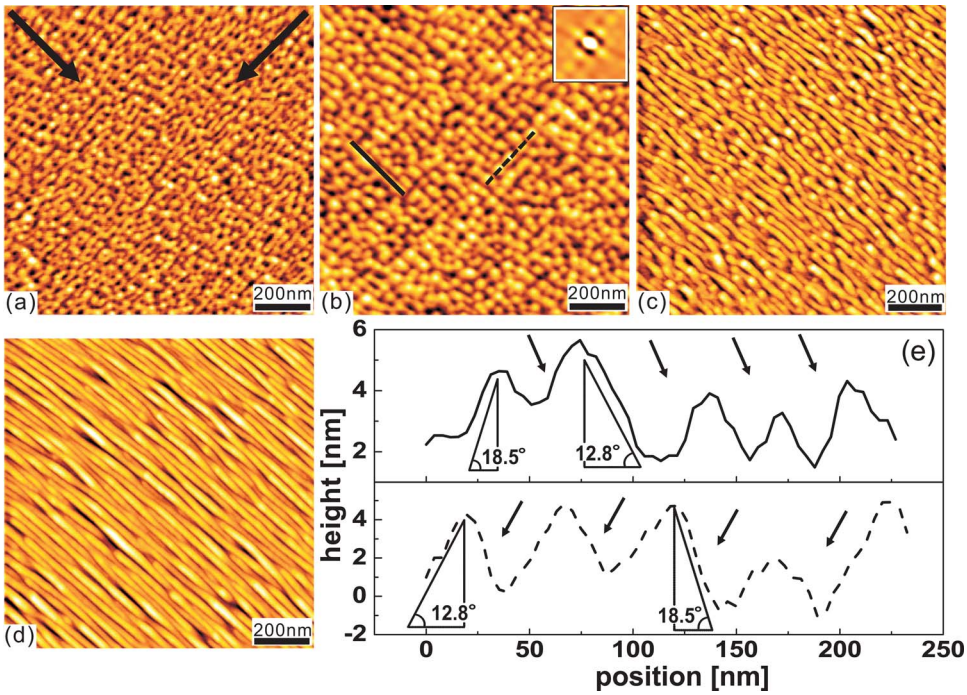

FIG. 2. (Color online) Surface morphologies induced by DIBS in the erosion regime in the order of increasing sputter time; (a) t=10 min, W=7.7 Å, and λ=37–45 nm. (b) t=32 min, W =19.0 Å, and λ=43–48 nm. (c) Modulated ripple at t=16 min under the condition of slight imbalance of fluxes; f_1 decreases by about 5%, while f_2 increases by about 30% with respect to (b). (d) Ripple induced by SIBS with the same flux f_2 with (c). (e) Height profiles along the lines marked in (b). The arrows in (a) and (e) indicate each ion-beam direction.

behaviors under the two sputtering conditions as follows. Each ion beam plays two contradictory roles: it constructs its own ripples and destroys the ripples formed by the crossing beam. If the two beams are not balanced, then one beam (major beam) breaks a crossing ripple into nanodots, while the other beam (minor beam) simply causes modulation of its crossing ripple and is incapable of breaking it into separate nanodots. Figure 2(c) shows the modulated ripple pattern formed under the sputtering condition, where the balance between the two beams is shifted slightly. The observed modulation is reminiscent of the incomplete breakage of the ripples into dots by the crossing (minor) ion beam. The modulated ripple is in sharp contrast to the ripple formed by single-ion-beam sputtering (SIBS), which shows no modulation in the height and width of each ripple [Fig. 2(d)].

In contrast, under the diffusion regime, the healing kinetics via the fast diffusion of adatoms and/or vacancies along the edges of the ripples are so efficient[9] that the ripples always maintain their shape, even under sputtering by the crossing ion beam. Hence, the ripple-bounded holes are observed under most sputtering conditions.

As the first attempt in understanding DIBS patterning, we applied the Sigmund theory to dual beam sputtering. The normal erosion velocity V_o at a generic point o on the surface is described simply by the superposition of the two energy dissipation functions corresponding to the two ion beams as follows: $V_o \propto \int d\mathbf{r}\{\varepsilon_1(\mathbf{r})f_1(\mathbf{r})+\varepsilon_2(\mathbf{r})f_2(\mathbf{r})\}$, where the dissipation of the impact energy $\varepsilon(\mathbf{r})$ is represented by a Gaussian function.[12,13] The obtained continuum equation for DIBS retains the same form as the KS equation when the azimuthal angle between the two incident beams is 90°. However, the coefficients of each term are altered. The coefficients ν and D of the $\nabla^2 h$ and $\nabla^4 h$ terms, respectively, are transformed as $\nu_x \rightarrow \nu_x^{(\mathrm{DIBS})}=\nu_x^{(x)}+r\nu_x^{(y)}$, where $\nu_i^{(x)}$ is the coefficient of the $\nabla_i^2 h$ term when a single ion beam is incident along the x direction, and $\nu_y \rightarrow \nu_y^{(\mathrm{DIBS})}=\nu_y^{(x)}+r\nu_y^{(y)}$, where $\nu_i^{(y)}$ is defined similarly, and $r=f_2/f_1$. D is transformed in the same manner; $D_{xx}^{(\mathrm{DIBS})}=D_{xx}^{(x)}+rD_{xx}^{(y)}$, where $D_{ii}^{(x)}$ is the coefficient of the $\nabla_{ii}^4 h$ term when a single ion beam is incident along the x direction, and i is either x or y. The numerical value of each coefficient is estimated using TRIM analysis[14] under the experimental conditions. Since $\nu_x^{(x)}$ and $\nu_y^{(y)}$ have very large positive values, the coefficients $\nu_x^{(\mathrm{DIBS})}$ and $\nu_y^{(\mathrm{DIBS})}$ become positive, although $\nu_x^{(y)}=\nu_y^{(x)}<0$. Also, $D_{xx}^{(\mathrm{DIBS})}=D_{yy}^{(\mathrm{DIBS})}<0$ although $D_{xx}^{(y)}=D_{yy}^{(x)}>0$. Therefore, the linear instability condition for the KS equation no longer holds for the DIBS, in contrast to the experimental observations. This indicates that processes beyond the scope of the KS equation govern the kinetics on the surface during DIBS.

To overcome this inconsistency, one may invoke the hydrodynamic model recently developed in Refs. 11 and 15. This model considers the redeposition effects of eroded atoms, which can diffuse on the surface isotropically. The resulting kinetic equation includes nonlinear terms of the form, $(\nabla h)^2$ and $\nabla^2(\nabla h)^2$ besides the linear terms, although the coefficients of each term are totally altered from the case in which the redeposition is not considered. For example, when the ion beam is incident in normal direction,[16] this approach yields the opposite sign[15] for the coefficient of the $\nabla^2(\nabla h)^2$ term to that obtained from the Sigmund approach.[17,18] Therefore, this approach may shed light on the instability observed by DIBS. Further study in this direction is under way.

To acquire further insight of the growth kinetics during DIBS,[19] we measure the surface roughness at each fluence, and obtain $\beta=0.35\pm0.06$ in the diffusion regime and $\beta=0.47\pm0.06$ in the erosion regime. These values are larger than the universal value $\beta\approx0.24$ for the Kadar-Parisi-Zhang equation and $\beta=0.16-0.25$ for the KS equation in two dimensions,[20] but supports the present argument that DIBS does not follow the KS equation. We note that our system has not reached stationary state even at the largest fluences reported. Furthermore, coarsening of nanostructures are clearly observed; wavelength (λ) increases from 37–43 nm in Fig. 1(c) to 52–68 nm in Fig. 1(d) in diffusion regime and from 37–45 nm in Fig. 2(a) to 43–48 nm in Fig. 2(b) in erosion regime.

We performed DIBS on Au(001) and studied the development of the induced pattern. DIBS formed highly ordered nanopatterns: 2D nanohole pattern in the diffusion regime and nanodot pattern in the erosion regime. The ordered pattern formation of the nanodots is very sensitive to the balance of the two ion beams. Slope asymmetry of nanostructures was induced by crossing ion beam during DIBS. We derived the KS equation from Sigmund theory to consider dual beam sputtering, which predicts a stable surface in contrary with the experimental observations. DIBS is a salient approach to sputter-induced pattern formation, and simultaneously raises challenging questions concerning the existing theoretical framework for our understanding of sputter-induced nanopatterning.

J.-S. Kim thanks Ziberi for informing the authors on the work of Carter. The work was supported by KOSEF (M10503000210-06M0300-21010) and a KOSEF grant funded by MOST (No. R17-2007-073-01001-0).

[1] S. Facsko, T. Dekorsy, C. Koerdt, C. Trappe, H. Kurz, A. Vogt, and H. L. Hartnagel, Science **285**, 1551 (1999).
[2] G. Constantini, F. Buatier de Mongeot, C. Boragno, and U. Valbusa, Phys. Rev. Lett. **86**, 838 (2001).
[3] E. Carrasco, O. Rodríguez de la Fuente, M. A. González, and J. M. Rojo, Eur. Phys. J. B **40**, 421 (2004).
[4] S. Rusponi, G. Costantini, C. Boragno, and U. Valbusa, Phys. Rev. Lett. **81**, 2735 (1998).
[5] C. C. Umbach, R. L. Headrick, and K.-C. Chang, Phys. Rev. Lett. **87**, 246104 (2001).
[6] A.-D. Brown, J. Erlebacher, W.-L. Chan, and E. Chason, Phys. Rev. Lett. **95**, 056101 (2005).
[7] G. Carter, Vacuum **77**, 97 (2004).
[8] S. Vogel and S. J. Linz, Phys. Rev. B **75**, 085425 (2007).
[9] U. Valbusa, C. Boragno, and F. Buatier de Mongeot, Mater. Sci. Eng., C **23**, 201 (2003).
[10] S. Park, B. Kahng, H. Jeong, and A.-L. Barabási, Phys. Rev. Lett. **83**, 3486 (1999).
[11] J. Muñoz-García, M. Castro, and R. Cuerno, Phys. Rev. Lett. **96**, 086101 (2006).
[12] P. Sigmund, Phys. Rev. **184**, 383 (1969).
[13] M. A. Makeev, R. Cuerno, and A.-L. Barabási, Nucl. Instrum. Methods Phys. Res. B **197**, 185 (2002).
[14] See http://www.srim.org for TRIM analysis.
[15] M. Castro, R. Cuerno, L. Vázquez, and R. Gago, Phys. Rev. Lett. **94**, 016102 (2005).
[16] T. C. Kim, C.-M. Ghim, H. J. Kim, D. H. Kim, D. Y. Noh, N. D. Kim, J. W. Chung, J. S. Yang, Y. J. Chang, T. W. Noh, B. Kahng, and J.-S. Kim, Phys. Rev. Lett. **92**, 246104 (2004).
[17] M. Castro and R. Cuerno, Phys. Rev. Lett. **94**, 139601 (2005).
[18] T. C. Kim, Phys. Rev. Lett. **94**, 139602 (2005).
[19] A.-L. Barabási and H. E. Stanley, *Fractal Concepts in Surface Growth* (Cambridge University Press, Cambridge, 1995).
[20] J. T. Drotar, Y.-P. Zhao, T.-M. Lu, and G.-C. Wang, Phys. Rev. E **59**, 177 (1999).